Applied Physics B (2023) 129:86
https://doi.org/10.1007/s00340-023-08032-9

Applied Physics B
Lasers and Optics

RESEARCH

Spectral broadening of a burst-mode 100 W Nd-doped picosecond amplifier in a multi-pass cell device

Jiajun Song[1] · Yujie Peng[1] · Guangxin Luo[1,2] · Liya Shen[1,3] · Jianyu Sun[1,4] · Yinfen Liu[1,4] · Yuxin Leng[1]

Received: 7 March 2023 / Accepted: 28 April 2023 / Published online: 8 May 2023

Abstract
The pulse duration of a burst-mode 100 W Nd-doped picosecond amplifier is nonlinearly compressed in a multi-pass cell device. The spectral broadening and pulse compression are investigated theoretically. The spectral bandwidth is broadened from 0.13 to 3.28 nm experimentally, corresponding to a broadening factor of 25.2. The pulse duration is compressed from 14.2 to 0.99 ps, corresponding to a compression factor of 14.3. The compressed pulse duration of four successive pulses are theoretically estimated to be 0.98 ps, 1.47 ps, 1.86 ps, and 3.07 ps, respectively. The laser power after the grating pair compressor is 72 W. Therefore, the total efficiency of our system reaches 72%. The beam quality after the MPC unit is almost preserved with a M^2 value of 1.38×1.40.

1 Introduction

High power ultrafast lasers are powerful tools for the research of material processing, such as the generation of 3D microstructures [1], the ablation of high polymer material [2, 3], and laser deposition [4]. Compared with single pulse mode, ultrafast lasers with burst-mode possess improved quality and higher removal rates during the microfabrication process [2]. The burst-mode ultrafast lasers also have the potential to be applied in biomedical and energy fields, like thrombus ablation [5] and the cutting of material for the Li-ion battery [6]. Therefore, improving the properties of the burst-mode ultrafast lasers makes significant sense for practical applications. The pulse duration is one of the core parameters of the ultrafast lasers. Ti: Sapphire ultrafast lasers can radiate ~ 30 fs pulses directly, but the available pump sources and large quantum defects of the Ti: Sapphire crystals severely limit the repetition rate of the Ti: Sapphire amplifier to ~ kHz and average power to 20 W level [7, 8]. Ytterbium (Yb)-doped bulk gain media such as Yb: KYW [9, 10], Yb: KGW [11], Yb: CALGO [12, 13], Yb: CaF_2 [14] and Yb: $CaYAlO_4$ [15] can radiate laser pulses of around 200 fs. Furthermore, Yb-doped gain media possess the advantages of low quantum defects and can be directly pumped with the high-power laser diode (LD). Therefore, Yb-doped high-power femtosecond lasers have developed rapidly in the last few years. Nevertheless, the chirped pulse amplification (CPA) technology could be applied to boost the pulse energy of the Yb-doped ultrafast lasers. Hence, high-power Yb-doped amplifiers suffer bulky configurations.

The neodymium (Nd)-doped gain media such as Nd: YVO_4 and Nd: YAG also possess the low quantum defects and can be directly pumped with high-power LD. Limited by emission spectral bandwidth, the pulse duration of the Nd-doped picosecond amplifier is typically around 10 ps, which means that the temporal stretcher and compressor can be omitted in the Nd-doped picosecond amplifiers. Hence, the Nd-doped picosecond lasers possess simple configuration and small footprint. By combining the high-power Nd-doped picosecond amplifiers with nonlinear post-compression technologies, it is more feasible to obtain high-power ultrafast

✉ Yujie Peng
yjpeng@siom.ac.cn

✉ Yuxin Leng
lengyuxin@mail.siom.ac.cn

[1] State Key Laboratory of High Field Laser Physics and CAS Center for Excellence in Ultra-Intense Laser Science, Shanghai Institute of Optics and Fine Mechanics (SIOM), Chinese Academy of Sciences (CAS), Shanghai 201800, China

[2] Department of Optics and Optical Engineering, University of Science and Technology of China, Hefei 230026, China

[3] School of Physical Science and Technology, ShanghaiTech University, Shanghai 201210, China

[4] Center of Materials Science and Optoelectronics Engineering, University of Chinese Academy of Sciences, Beijing 100049, China

lasers with the same merit as the Nd-doped picosecond lasers but with a shorter pulse duration.

A variety of post-compression techniques have been demonstrated, such as solid core fiber [16], gas-filled Kagome hollow-core PCF [17], hollow core fiber [18], solid thin plates [19–21] and Multi-Pass Cell (MPC) [22–27]. For a 100 W level commercially available picosecond amplifier, it has a typical pulse duration of ~ 10 ps and a repetition rate of several hundred kilohertz. Hence, the peak power of the high-power picosecond laser is at 10 MW level. In [22], we have summarized the input laser pulse parameters applicable to different post-compression devices. It is clear that the MPC is the most ideal scheme for post-compression of high-power picosecond pulses. Since it distributes the nonlinear spectral broadening in multiple steps, the self-focusing or spatial–temporal coupling is negligible, and the beam quality is almost preserved. The MPC also features low cost, high efficiency, and compact configuration. To sum up, the MPC is the most applicable technology for post-compression of the burst-mode high-power Nd-doped picosecond lasers.

The laser pulses within a burst are amplified one after another. As a result, the pulse energies within a burst decrease sequentially. During the nonlinear interactions, the pulses will undergo different spectral broadening, so the group delay dispersion (GDD) required to compress the pulses to the Fourier transform limit (FTL) is different. Since the pulses within a burst are dispersion compensated simultaneously, the compressed pulse durations will be different. Therefore, it is essential to compensate for the proper amount of GDD to ensure that all pulses have excellent temporal quality.

In this letter, we demonstrate the simulations of the spectral broadening and pulse compression of a 100 W burst-mode Nd-doped picosecond amplifier. Also, on the experiment the spectral bandwidth of the driving laser is broadened from 0.13 to 3.28 nm, corresponding to a spectral broadening factor of 25.2. After dispersion compensation, we estimate the compressed pulse durations of four successive pulses are 0.98 ps, 1.47 ps, 1.86 ps, and 3.07 ps, respectively. And all pulses are not split, theoretically.

2 Experimental setup

The experimental setup is depicted in Fig. 1a. An Nd-doped burst-mode picosecond amplifier is employed as the driving source. It consists of a 20 MHz mode-locked picosecond oscillator, a pulse picker, and multi-stage amplifiers. The driving source delivers an average power of 100 W at a repetition rate of 200 kHz. Each burst contains four pulses by controlling the gate width of the pulse picker. The four pulses are amplified one after another, so their energy decreases sequentially. The energy ratio between the four pulses is collected by a photodiode and monitored by an oscilloscope, and the result is 1:0.8:0.69:0.55, as presented in Fig. 1b. Thus, the energy of the 4 pulses within a burst are estimated to be 165 μJ, 130 μJ, 115 μJ and 90 μJ, respectively. The pulse duration of the picosecond laser is 14.2 ps (full width at half maximum, FWHM) assuming a $Sech^2$ pulse shape, as shown in Fig. 1c. Assuming that all pulse energy is contained in the main peak, the peak powers of the four pulses are 10.2 MW, 8.0 MW, 7.1 MW, and 5.6 MW, respectively. The central wavelength and spectral bandwidth (FWHM) of the picosecond laser are 1064.4 nm and 0.13 nm respectively, as presented in Fig. 1d. The MPC consists of two concave mirrors (CM1–CM2) with a

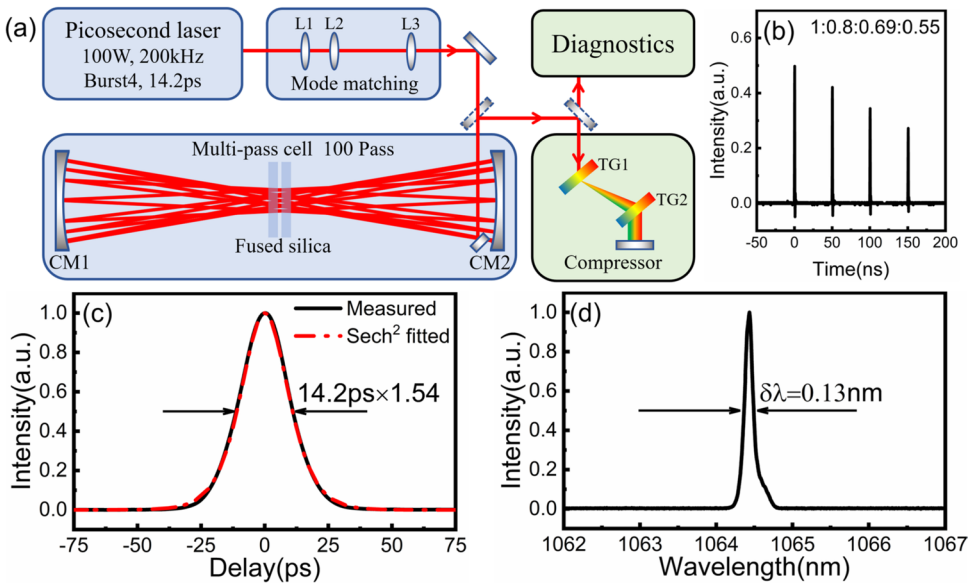

Fig. 1 **a** Experimental setup. L1–L3, lenses, CM1–CM2, concave mirrors, TG1–TG2, transmission gratings. **b** Burst pulse trains, **c** Measured intensity autocorrelation trace (black line) and $Sech^2$ fit (red line). **d** Spectrum of the picosecond laser

diameter of 76.2 mm and a radius of curvature of 300 mm. The concave surfaces are coated with a high reflection coating at 1064 nm with a reflectivity higher than 99.9%. The distance between the CM1 and CM2 is set to approximately 530 mm, corresponding to an eigenmode radius of 529 mm on the MPC mirrors and 181 mm in the middle of the MPC. The mode matching between the picosecond laser and the MPC is realized through three lenses (L1–L3). Two 9 mm thick fused silica plates are employed as the Kerr-mediums, which are positioned in the middle of the MPC. The laser beam injection and extraction from the MPC is executed by a rectangular mirror with a width of 3 mm. The picosecond laser beam is aligned to propagate 50 roundtrips inside the MPC, corresponding to 100 passes through the plates. Thus, the total distance propagated in fused silica and in free-space is about 1.8 m and 51.2 m, respectively. A Treacy-type compressor consisting of two 1200 grooves/mm transmission gratings (TG1–TG2) is employed to compensate for the positive chirp induced by the self-phase modulation (SPM).

3 Results and discussion

At 100 W of full power input, the output power of the MPC is 83 W, corresponding to an efficiency of 83%. The loss arises from 99 reflections on the MPC mirrors and 100 passes through the plates. Since the peak powers of the four pulses are different, they will accumulate different nonlinear phase shifts as they propagate through the MPC unit, which means that the spectra of the four pulses output from the MPC will be clearly different. Eventually, the negative GDD required to compress the four pulses to the Fourier transformation limit (FTL) is different. Therefore, theoretical simulations are necessary to evaluate the spectral broadening and pulse compression results. The spectral broadening and pulse compression of the picosecond pulses in the MPC can be simulated by solving the generalized nonlinear Schrödinger equation [28].

Figure 2a–d shows the theoretically calculated broadened spectra of the four pulses within a burst. It is clear that the spectra expand almost symmetrically to both sides, with a series of peaks. Hence, in our experimental terms, the spectral broadening is dominate by the SPM effect. As the peak power of the four pulses decreases progressively, so does the nonlinear phase shift. The calculated spectral bandwidths of the four pulses at the intensity of half the outer spectral maxima are 2.73 nm, 2.15 nm, 1.90 nm, and 1.47 nm, respectively. Correspondingly, the FTL pulse durations of the calculated broadened spectra are 0.94 ps, 1.17 ps, 1.3 ps, and 1.62 ps respectively, as depicted on the right side of Fig. 2a–d.

The envelopes of the Nd-doped picosecond pulses from the MPC are almost preserved, but all with a positive chirp. With precision dispersion compensation, the pulse duration will be significantly shorter than the initial input picosecond laser. The variation of the pulses with compensated negative GDD is simulated theoretically, as shown in Fig. 3a–d. It is clear that the amount of GDD required to compress the four successive pulses to FTL gradually increases. For the first pulse, when the compensated GDD reaches – 1.7 ps^2, it is compressed close to the FTL firstly. Increasing the compensated GDD to – 2.5 ps^2, the intensity of the side pulses progressively increase. And the first pulse will split into several peaks if further increase in GDD compensate for

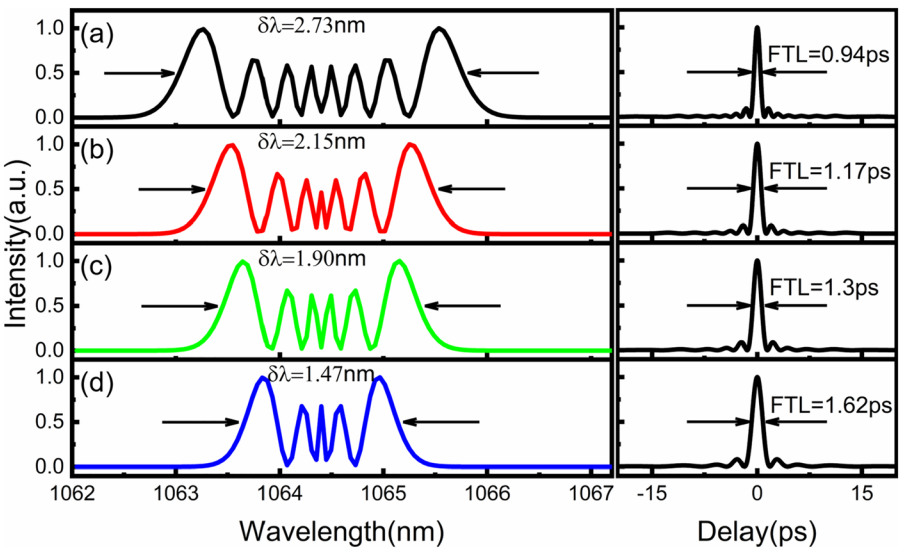

Fig. 2 Theoretical calculated spectral broadening results. **a–d** Burst1–4. Right side, corresponding FTL pulse duration

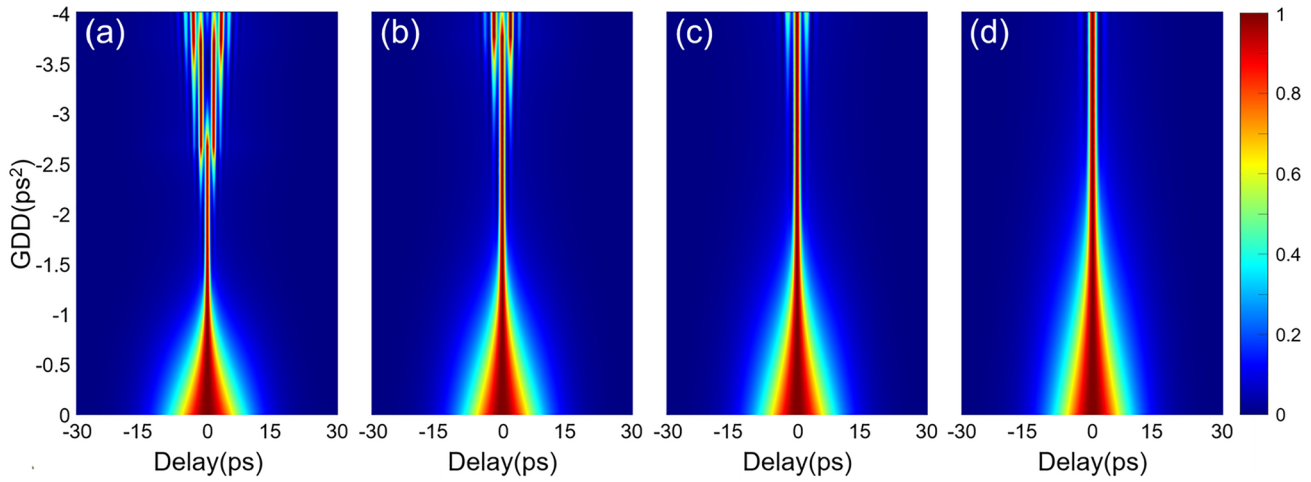

Fig. 3 Variation of the pulse shape with compensated GDD. **a–d** The first pulse to fourth pulse in a burst

this. For the 2-4th pulses, the amount of GDD required to compress the pulse to an ideal pulse shape is approximately – 2.2 ps^2, – 2.5 ps^2, and – 3.2 ps^2, respectively. Our definition of the ideal compression result is that the intensity of the side pulses are as low as possible and the main peak of the compression pulse is close to the FTL. Since the energy is mainly concentrated in the first pulse (33%), we consider that none of the pulses split and the first pulse is close to the FTL to be an ideal compression scheme. Therefore, the amount of compensated GDD should be approximately – 1.7 ps^2, theoretically.

The broadened spectrum from the MPC unit is monitored by a high-resolution optical spectrum analyzer (AQ6374, YOKOGAWA), the result presented in Fig. 4a. The broadened spectrum possesses a multi-peak structure, which suggests that the spectral broadening within the MPC unit is indeed dominated by the SPM. The number of peaks in the broadened spectrum is significantly more than the theoretically calculated spectra of the first pulse. This is because the measured spectrum is a total superposition of the broadened spectra of the four pulses, which means that the peaks of the measured spectrum may come from different pulses. The spectral bandwidth of the broadened spectrum is 3.24 nm (taken at half the intensity of the outer spectral maxima), corresponding to a broadening factor of 25.2. The FTL of the broadened spectrum is calculated to be 0.93 ps, as shown in the inset of Fig. 4a. Then the pulses are injected into the compressor to remove the positive chirp. The laser beam is incident on the TG at a Littrow angle of 39.7° for maximizing diffraction efficiency. The average power of the picosecond laser after the compressor is 72 W, corresponding to a compression efficiency of 86.7%. The compressed pulse duration is characterized by a commercial intensity autocorrelator (A.P.E. Pulse check-150). By fine tuning the distance between the TG1 and TG2, a shortest 1.35 ps autocorrelation trace is measured, as shown in Fig. 4b (black line). At this point, the distance between the TG1 and TG2 is 12 cm, and the GDD that can compensate is about – 1.62

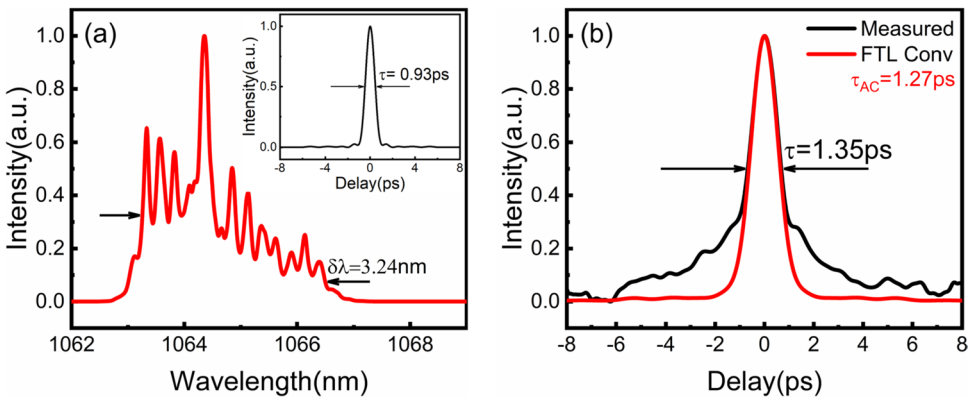

Fig. 4 **a** The measured broadened spectrum. Inset, FTL of the broadened spectrum. **b** Compressed intensity autocorrelation trace (black curve) and the convolution of the FTL pulse (red curve)

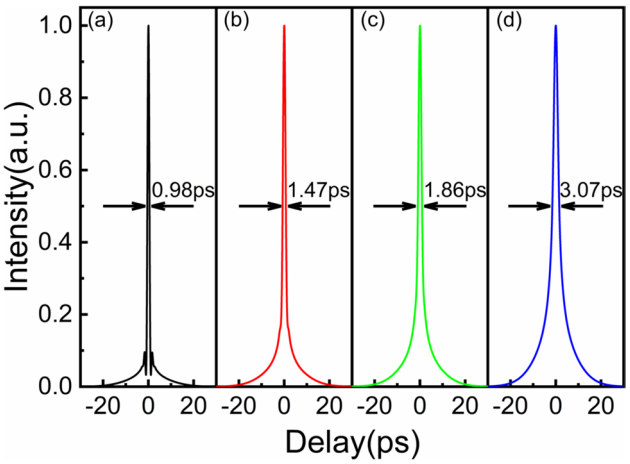

Fig. 5 Theoretically calculated pulse duration of four successive pulses when compensating for the GDD of – 1.62 ps^2. **a**–**d** The first pulse to fourth pulse in a burst

ps^2. The simulated autocorrelation trace of the FTL pulse is 1.27 ps, as presented in Fig. 4b (red line). Assuming that the deconvolution factor of the compressed pulse is the same as the FTL (0.73), which yields an approximate compressed pulse duration of 0.99 ps. As mentioned before, the pulse durations of the four pulses are different when compensating for the same GDD. Hence, the measured intensity autocorrelation trace is not the real pulse duration of the four pulses. Figure 3a–d shows the theoretically calculated pulse durations for compensating different dispersion. We extracted the four pulse shapes from Fig. 3a–d for a compensated GDD of – 1.62 ps^2, as shown in Fig. 5a–d. The pulse durations of four successive pulses after the compressor are estimated to be 0.98 ps, 1.47 ps, 1.86 ps, and 3.07 ps, respectively, and four pulses are not split. Nevertheless, it is clear that the simulated four compressed pulse durations are different and all pulses contain macroscopic pedestal. By integration, we estimate the pulse energy contained in the main peaks of the four pulses as 54%, 55%, 56%, and 65%, respectively. Although the first pulse is near the FTL, its main peak contains the least amount of pulse energy due to the broadened spectrum has more intensity modulation. As a comparison, the subsequent pulses feature better temporal quality, although they are farther from the FTL due to insufficient dispersion compensation. By employing a burst-mode picosecond laser with consistent pulse energies as the driving source, coincident pulse compression results are expected, both in terms of compressed pulse duration and temporal quality.

Figure 6a, b presents the beam quality (M^2) of the picosecond laser before and after the MPC unit. The beam quality after the MPC is basically preserved with a M^2 values of 1.38×1.40.

4 Conclusion

In conclusion, post-compression of a 100 W burst-mode Nd-doped picosecond amplifier in a solid-state MPC unit is demonstrated. For the pulses with different pulse energy, the theoretical simulation to evaluate the spectral broadening and pulse compression is implemented. To ensure the four pulses after chirp removal are not split, only the first pulse is compressed to near FTL, 2nd–4th pulses are still positively chirped. The theoretically calculated compressed pulse durations of four pulses are 0.98 ps, 1.47 ps, 1.86 ps, and 3.07 ps, respectively. The total efficiency of the optical system reaches 72%, while the beam quality of the driving laser after the MPC is almost preserved with a M^2 value of 1.38×1.40. Due to the non-adjustable energy ratio between the four pulses, the actual compressed pulse

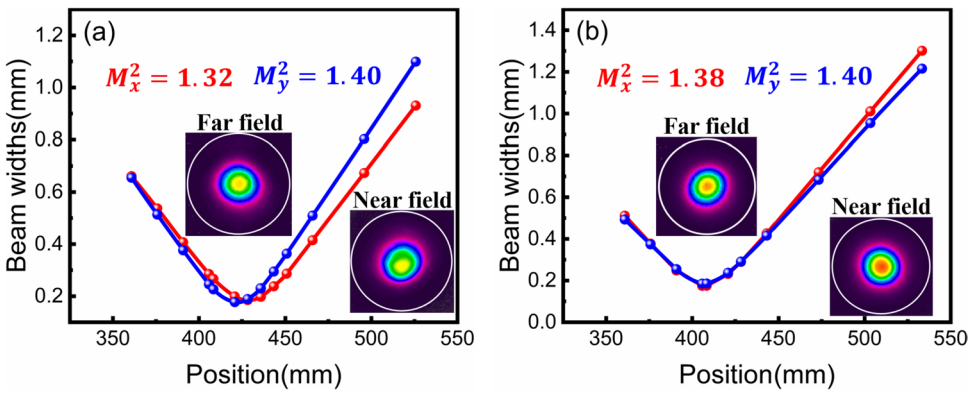

Fig. 6 Beam quality (M^2) of the burst-mode picosecond laser. **a** Before the MPC unit, **b** After the MPC unit

duration is different, while more pulse energy contained in the uncompressed pedestal. Using a burst-mode picosecond laser with consistent pulse energy as the driving source, the same pulse compression results are expected, both in terms of compressed pulse duration and temporal quality. This laser source has great potential to be applied in microfabrication field.

Acknowledgements This work was supported by National Natural Science Foundation of China (61925507, 62075227, 62205351, 22227901), Shanghai Rising-Star Program (21QA1410200), Youth Innovation Promotion Association CAS (2020248).

Author contributions JS, YP and YL contributed to the design and experimental schemes. JS, GL, LS, YL and JS performed the experiments and are responsible for the data processing. JS, YP and LS contributed to write and edit the manuscript. All authors reviewed the manuscript.

Funding National Natural Science Foundation of China, 61925507, 62075227, 62205351, 22227901, Shanghai Rising-Star Program, 21QA1410200, Youth Innovation Promotion Association of the Chinese Academy of Sciences, 2020248.

Data availability Data underlying the results presented in this paper are not publicly available at this time but may be obtained from the authors upon reasonable request.

Declarations

Conflict of interest The authors declare that there is no conflict of interest.

References

1. P. Lickschat, D. Metzner, S. Weissmantel, Manufacturing of high quality 3D microstructures in stainless steel with ultrashort laser pulses using different burst modes. J. Laser Appl. **33**(4), 042002 (2021)
2. J. Molinuevo, E. Rodriguez-Vidal, I. Quintana, M. Morales, C. Molpeceres, Experimental investigation into ultrafast laser ablation of polypropylene by burst and single pulse modes. Opt. Laser Technol. **152**, 108098 (2022)
3. D. Metzner, P. Lickschat, A. Engel, T. Lampke, S. Weissmantel, Ablation characteristics on silicon from ultrafast laser radiation containing single MHz and GHz burst pulses. Appl. Phys. Mater. Sci. Process. **128**(8), 723 (2022)
4. S.J. Dai, J. Yu, J.G. He, Y. Liu, Z.Q. Mo, E.L. Wu, J.J. Meng, Improvement of Al thin film morphology with picosecond pulsed laser deposition in burst mode. Appl. Phys. Express **14**(7), 075501 (2021)
5. H.T. Zhang, X.Z. Liu, Y.N. Li, W.W. Wu, Y. Gu, T. Zhang, Study on the mechanism of thrombus ablation in vitro by burst-mode femtosecond laser. J. Biophotonics **15**(11), e202200197 (2022)
6. J.Y. Huang, W.Q. Shi, J. Huang, Y.P. Xie, Y. Ba, K.F. He, High speed pulsed laser cutting of anode material for a Li-ion battery in burst mode. Opt. Mater. Express **11**, 2300–2309 (2021)
7. V. Bagnoud, F. Salin, Amplifying laser pulses to the terawatt level at a 1-kilohertz repetition rate. Appl. Phys. B **70**, S165–S170 (2000)
8. B. Langdon, J. Garlick, X. Ren, D.J. Wilson, A.M. Summers, S. Zigo, M.F. Kling, S. Lei, C.G. Elles, E. Wells, E.D. Poliakoff, K.D. Carnes, V. Kumarappan, I. Ben-Itzhak, C.A. Trallero-Herrero, Carrier-envelope-phase stabilized terawatt class laser at 1 kHz with a wavelength tunable option. Opt. Express **23**, 4563–4572 (2015)
9. A.L. Calendron, H. Cankaya, F.X. Kartner, High-energy kHz Yb:KYW dual-crystal regenerative amplifier. Opt. Express **22**, 24752–24762 (2014)
10. G.H. Kim, J. Yang, S.A. Chizhov, E.G. Sall, A.V. Kulik, V.E. Yashin, D.S. Lee, U. Kang, High average-power ultrafast CPA Yb:KYW laser system with dual-slab amplifier. Opt. Express **20**, 3434–3442 (2012)
11. H.J. He, J. Yu, W.T. Zhu, X.Y. Guo, C.T. Zhou, S.C. Ruan, A Yb:KGW dual-crystal regenerative amplifier. High Power Laser Sci. Eng. **8**, e35 (2020)
12. W.Z. Wang, T. Pu, H. Wu, Y. Li, R. Wang, B.A. Sun, H.K. Liang, High-power Yb:CALGO regenerative amplifier and 30 fs output via multi-plate compression. Opt. Express **30**, 22153–22160 (2022)
13. W.Z. Wang, H. Wu, C. Liu, B.A. Sun, H.K. Liang, Multigigawatt 50 fs Yb:CALGO regenerative amplifier system with 11 W average power and mid-infrared generation. Photonics Res. **9**, 1439–1445 (2021)
14. S. Ricaud, F. Druon, D.N. Papadopoulos, P. Camy, J.L. Doualan, R. Moncorge, M. Delaigue, Y. Zaouter, A. Courjaud, P. Georges, E. Mottay, Short-pulse and high-repetition-rate diode-pumped Yb:CaF2 regenerative amplifier. Opt. Lett. **35**, 2415–2417 (2010)
15. A. Rudenkov, V. Kisel, A. Yasukevich, K. Hovhannesyan, A. Petrosyan, N. Kuleshov, Yb3+:CaYAlO4-based chirped pulse regenerative amplifier. Opt. Lett. **41**, 2249–2252 (2016)
16. M. Seidel, X. Xiao, A. Hartung, Solid-core fiber spectral broadening at its limits. IEEE J. Sel. Top. Quantum Electron. **24**(5), 1–8 (2018)
17. F. Emaury, C.F. Dutin, C.J. Saraceno, M. Trant, O.H. Heckl, Y.Y. Wang, C. Schriber, F. Gerome, T. Sudmeyer, F. Benabid, U. Keller, Beam delivery and pulse compression to sub-50 fs of a modelocked thin-disk laser in a gas-filled Kagome-type HC-PCF fiber. Opt. Express **21**, 4986–4994 (2013)
18. S. Bohman, A. Suda, T. Kanai, S. Yamaguchi, K. Midorikawa, Generation of 5.0 fs, 5.0 mJ pulses at 1 kHz using hollow-fiber pulse compression. Opt. Lett. **35**, 1887–1889 (2010)
19. P. He, Y.Y. Liu, K. Zhao, H. Teng, X.K. He, P. Huang, H.D. Huang, S.Y. Zhong, Y.J. Jiang, S.B. Fang, X. Hou, Z.Y. Wei, High-efficiency supercontinuum generation in solid thin plates at 0.1 TW level. Opt. Lett. **42**, 474–477 (2017)
20. M. Seo, K. Tsendsuren, S. Mitra, M. Kling, D. Kim, High-contrast, intense single-cycle pulses from an all thin-solid-plate setup. Opt. Lett. **45**, 367–370 (2020)
21. C.H. Lu, Y.J. Tsou, H.Y. Chen, B.H. Chen, Y.C. Cheng, S.D. Yang, M.C. Chen, C.C. Hsu, A.H. Kung, Generation of intense supercontinuum in condensed media. Optica **1**, 400–406 (2014)
22. J. Song, Z. Wang, R. Lv, X. Wang, H. Teng, J. Zhu, Z. Wei, Generation of 172 fs pulse from a Nd: YVO_4 picosecond laser by using multi-pass-cell technique. Appl. Phys. B **127**, 50 (2021)
23. J. Schulte, T. Sartorius, J. Weitenberg, A. Vernaleken, P. Russbueldt, Nonlinear pulse compression in a multi-pass cell. Opt. Lett. **41**, 4511–4514 (2016)
24. A.L. Viotti, S. Alisauskas, H. Tunnermann, E. Escoto, M. Seidel, K. Dudde, B. Manschwetus, I. Hartl, C.M. Heyl, Temporal pulse quality of a Yb:YAG burst-mode laser post-compressed in a multi-pass cell. Opt. Lett. **46**, 4686–4689 (2021)
25. E. Escoto, A.L. Viotti, S. Alisauskas, H. Tunnermann, I. Hartl, C.M. Heyl, Temporal quality of post-compressed pulses at large compression factors. J. Opt. Soc. Am. B-Opt. Phys. **39**, 1694–1702 (2022)
26. P. Balla, A. Bin-Wahid, I. Sytcevich, C. Guo, A.L. Viotti, L. Silletti, A. Cartella, S. Alisauskas, H. Tavakol, U. Grosse-Wortmann, A. Schonberg, M. Seidel, A. Trabattoni, B. Manschwetus, T. Lang, F. Calegari, A. Couairon, A. L'Huillier, C.L. Arnold, I. Hartl, C.M. Heyl, Postcompression of picosecond pulses into the few-cycle regime. Opt. Lett. **45**, 2572–2575 (2020)

27. M. Seidel, F. Pressacco, O. Akcaalan, T. Binhammer, J. Darvill, N. Ekanayake, M. Frede, U. Grosse-Wortmann, M. Heber, C.M. Heyl, D. Kutnyakhov, C. Li, C. Mohr, J. Muller, O. Puncken, H. Redlin, N. Schirmel, S. Schulz, A. Swiderski, H. Tavakol, H. Tunnermann, C. Vidoli, L. Wenthaus, N. Wind, L. Winkelmann, B. Manschwetus, I. Hartl, Ultrafast MHz-rate burst-mode pump-probe laser for the FLASH FEL facility based on nonlinear compression of ps-level pulses from an Yb-amplifier chain. Laser Photonics Rev. **16**(3), 2100268 (2022)
28. J.M. Dudley, G. Genty, S. Coen, Supercontinuum generation in photonic crystal fiber. Rev. Mod. Phys. **78**, 1135–1184 (2006)